2024 European Control Conference (ECC)
June 25-28, 2024. Stockholm, Sweden

Energy Demand of Vessels Depending on Current Wind Conditions*

Agnes U. Schubert, Robert Damerius and Torsten Jeinsch[1]

***Abstract*— The paper describes a method for estimating the energy consumption of a vessel as a function of the current wind conditions and surge velocity. Wind forces have a great influence on ship motion, especially at low speeds, e.g. in narrow waterways. Therefore, in order to minimize the energy required for maneuvering, attention must be paid to the wind and the pose of the vessel to the wind. Adjusting the speed can also contribute to lower energy consumption. The method is based on different models for the motion, wind and power consumption of the individual actuators of the vessel. A simulation environment was created to control heading and surge velocity to calculate the power demand at different constant wind speeds and angles. As an example, these models were developed for the research vessel *DENEB* derived from real world experiments. Developed models and results are presented.**

I. INTRODUCTION

Energy-efficient ship operations are becoming increasingly important for the shipping industry in order to reduce fuel consumption and emissions. Economic pressure, stricter environmental regulations and tourist aspects play a role in the shipowners considerations. Mainly due to fuel prices, more attention is being paid to operational performance and especially speed. A review identified speed reduction as the second best measure to reduce CO2 emissions achieving between 20 and 35 percent less per unit of freight transported, especially for longer overseas shipments [1]. A higher reduction potential was only found for the use of biofuels with up to 84%. In addition to wind and wave influence, Bentin et al. [2] also investigates a weather routing tool that aims to minimize energy consumption while maintaining a maximum travel time. The result for a North Atlantic route shows a savings of $4-8$ %. In manoeuvring mode, the diesel engines are not operated at the working point, but are in a transient state most of the time, resulting in low efficiency and increased emissions, especially soot and NO_x [3]. But the thermodynamic processes in the engine are difficult to model, so estimates are usually used.

* The work was funded by the German Federal Ministry of Economic Affairs and Climate Action (BMWK), supported by the DLR Space Administration and the German Federal Maritime and Hydrographic Agency (BSH) under the registration number FKZ 50NA2304B as well as by the German Federal Ministry for Digital and Transport (BMDV) under FKZ 03RU1U012I.

[1]The Authors are with Institute of Automation, Faculty of Computer Science and Electrical Engineering, University of Rostock, Germany agnes.schubert@uni-rostock.de

Further, there is a shortage of skilled workers in the nautical sector in particular because of aging. For this reason, Japan is aiming 50% autonomous coastal shipping in 2040 through the MEGURI2040 project [4]. Both trends, more efficient operation and a lack of skilled personnel, lead to increased efforts to establish assistive and automated functionalities on board ships. The challenges are especially great when maneuvering in narrow waterways or near structures.

The influence of environmental forces increases when a ship maneuvers at low speeds [5]. Experienced officers can assess whether a ship is still maneuverable under certain weather conditions with the available propulsion configuration or which maneuver strategy will safely lead to the destination. A strict schedule of ferries additionally requires high precision in maneuvering. In order to support efficient and precise maneuvering via assistance systems or automatic operations, a known influence of wind forces is essential, also for minimizing energy consumption or designing maneuvering strategies.

There are numerous scientific and industrial publications about automated maneuvering under wind disturbances. The most of them address the control quality for automatic berthing maneuvers. A pure pursuit algorithm for automatic berthing of a boat was adapted in [5]. The path following control is combined with heading and velocity control including wind forces in the basic motion model. The approach of [6] is using an artificial neural network in combination with a PD heading controller for an automatic berthing maneuver of a model ship, where the influence of low wind speeds from different directions are considered. An example with more focus on assistance for conventional manual control onboard a Korean training ship can be found in [7]. Drift and counter rudder angle due to wind effect are calculated with a static equilibrium method in order to determine the critical wind velocity. At low speed in port areas, the bow thruster is used in addition to the rudder.

This paper provides a method to quantify the influence of current wind conditions on the energy consumption of a ship while maneuvering in safety-critical areas, e.g., ports. The potential adjustment of the surge velocity is considered. The approach is based on models of motion behavior, actuator and wind forces as well as the resulting energy demand. These models were developed as an example for the 52 m long research vessel *DENEB* by different maneuvers in the real world. The aim of the investigations was to estimate the energy requirements

of newly built light ships with limited energy capacity. Depending on the different wind conditions that occur on a defined route over the course of a year, the energy capacities with reserve should be designed accordingly. The scope of the vessels is limited to shorter ferry routes, where maneuvering at lower speeds takes up a large part of the total distance.

II. MODEL DEVELOPMENT

Three ship-specific models are required to estimate the energy demand under current wind conditions, the motion model, the wind model, and the power curves of the individual propulsion systems. This structure is shown in Fig. 1. The vector sum of external forces, such as the wind forces and actuator forces produces the ship motion. For conventional vessels not designed for dynamic positioning (DP) operation, a motion model in three degrees of freedom (DoF) is generally sufficient. Neglecting the forces from the environment, this model dynamically reproduces the effect of the commanded manipulated variables for the actuators on the state variables of the motion process. The wind model considers areas and shapes of the vessel over water to calculate the wind effect on the vessel motion for measured or estimated wind conditions. Each actuator on the ship is characterized by its own power curve, which is essentially dependent on the rotational speed but also on the current motion states. All experiments are conducted with the research vessel *DENEB* in a restricted area of the Naval base in port of Rostock, where moderate environmental conditions are found, with the exception of the coasting stop maneuvers, for which areas outside the port were used.

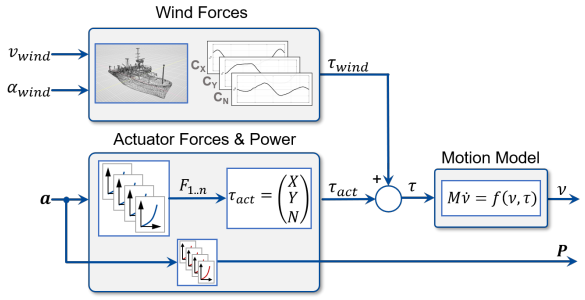

Fig. 1. Model structure with the particular modules for wind forces, actuator forces and motion

A. Motion Model and Actuator Forces

The motion model is based on Newton's second law referenced in [8] with

$$\boldsymbol{M}\dot{\boldsymbol{\nu}} + \boldsymbol{C}(\boldsymbol{\nu})\boldsymbol{\nu} = \boldsymbol{D}(\boldsymbol{\nu})\boldsymbol{\nu} + \boldsymbol{\tau} \tag{1}$$

where $\boldsymbol{M}$ is the inertia matrix, $\boldsymbol{\nu}$ is the velocity vector, $\boldsymbol{D}$ and $\boldsymbol{C}$ are the damping and the Coriolis and centripedal matrices, and $\boldsymbol{\tau}$ is the vector of external forces. It is calculated from the sum of the actuators thrust $\boldsymbol{\tau}_{act}$ and the wind forces $\boldsymbol{\tau}_{wind}$ for a model in three DoF to

$$\boldsymbol{\tau} = \begin{pmatrix} X, & Y, & N \end{pmatrix}^T = \boldsymbol{\tau}_{act} + \boldsymbol{\tau}_{wind} \tag{2}$$

where X and Y are the forces in longitudinal and lateral direction and N is the yaw moment . The velocity vector is given by

$$\boldsymbol{\nu} = \begin{pmatrix} u, & v, & r \end{pmatrix}^T \tag{3}$$

with the surge velocity u, the sway velocity v and the yaw rate r. Since identification of the model parameters is very time-consuming and will nevertheless always remain inaccurate due to the numerous influencing factors, virtual forces were introduced for the effect of the actuators. Each actuator contributes a thrust amount to the total force $\boldsymbol{\tau_{act}}$ depending on the possible direction of its thrust. The generated moment also depends on the position of the respective actuator in relation to the ship's center of gravity (CG).

In order to identify the forces and moments of a given actuator configuration, a successive approach was chosen. It starts with the identification of the motion limited to the longitudinal direction by a single actuator. For this purpose, several coasting stops are performed to minimize the error in identification. In the result, a function

$$m\dot{u} = f(u, X) \tag{4}$$

is derived where m denotes the effective mass. This mass is only a gain factor for the virtual forces and can therefore be estimated with the mass given in the wheel house poster or from the displacement of the CAD model. The thrusts of the other actuators are determined in relation to this initially estimated force, in which force equilibrium is generated in one of the DoFs, so that there is no motion in this direction. The same reference frame is chosen for the wind.

The 52 m long research vessel *DENEB* has a diesel-electric propulsion system and four actuators arranged along the longitudinal axis of the ship, the main propulsion, rudder, a thruster in the stern as well as a pump-jet in the bow. Since it is intended for surveys and wreck search, the sensor equipment is significantly better than on conventional cargo ships. For example, a high-performance inertial navigation system (INS) is available. For the purpose of research, a digitization of the ship has been implemented early in 2021 to be able to control the drives automatically [10].

For this vessel, the input vector is thus given by

$$\boldsymbol{a} = \begin{pmatrix} e_M, & \delta_R, & e_{PJ}, & \delta_{PJ}, & e_T \end{pmatrix}^T \tag{5}$$

where the following denotations are introduced e_M the engine order telegraph (EOT) of the main propulsion, δ_R the rudder angle, e_{PJ} the EOT of the pump-jet, δ_{PJ} the angle of the pump-jet and e_T the EOT of the stern thruster. The geometric arrangement of the actuators is presented in Fig. 2. The main propulsion and the pump-jet can produce thrust in longitudinal direction, marked

with the forces F_1 and F_4. The combination of the main propulsion and rudder generates a transversal force F_5 as does the stern thruster with F_3 and the pump-jet with F_2 depending on the angle set. To estimate the three moments that can be generated by the forces F_5, F_3 and F_2, the corresponding distances along the longitudinal axis between CG and the respective actuator must be applied. The origin of the body-fixed coordinate system lies in CG. From these considerations follow the specific force vector with

$$\boldsymbol{\tau}_{act} = \begin{pmatrix} X \\ Y \\ N \end{pmatrix} = \begin{pmatrix} F_1 + F_4 \\ F_2 + F_3 + F_5 \\ L_1F_2 - L_2F_3 - L_3F_5 \end{pmatrix} \tag{6}$$

where L_1, L_2 and L_3 are the known distances between the actuator and CG, as illustrated in Fig. 2.

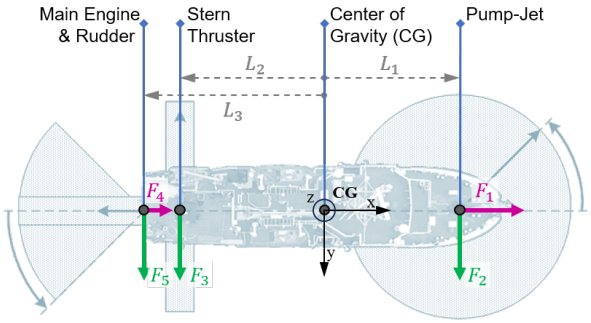

Fig. 2. Geometric arrangement of the actuators on the *DENEB*

Since the maximum producible force F_1 is also much lower than maximum F_4 and the pump-jet is the only propulsion unit in the vessel's bow, the thrust of the pump-jet was identified as the virtual basis of the reference frame. Coast stop maneuvers are conducted for the identification of this thrust. In Fig. 3, the u-plot of one of the coast stop maneuvers is presented. Care was taken to ensure that there was no motion in the transverse direction and around the vertical axis. The longitudinal motion of the three DoF model is modeled by the following differential equation

$$m\dot{u} = -d_u u - d_{uuu}u^3 + X \tag{7}$$

where d_u and d_{uuu} are the coefficients for the first and third order terms. In stationary case, $\dot{u} = 0$, the thrust X can be calculated from the commanded revolution speed e_{PJ} and a look-up table can be build.

In order to estimate the thrust of the other propulsion units, force equilibrium can be established with

$$F_4 = -F_1 \quad , \quad -L_2F_3 = L_1F_2 \quad , \quad -L_3F_5 = L_1F_2. \tag{8}$$

If there is no motion in the longitudinal direction, the thrust of the main propulsion F_4 can be determined from the state of equilibrium. In transversal direction, it is possible in the combinations of the pump-jet and stern thruster (F_2 and F_3) as well as the pump-jet and the coupled control of main propulsion and rudder (F_2 and F_5). This equilibrium must be set up in such a way that no rotational motion occurs, which is why the distances between the involved actuators and the CG must be taken into account. From the known thrust of each actuator, the force vector $\boldsymbol{\tau}_{act}$ can be calculated according equation 6.

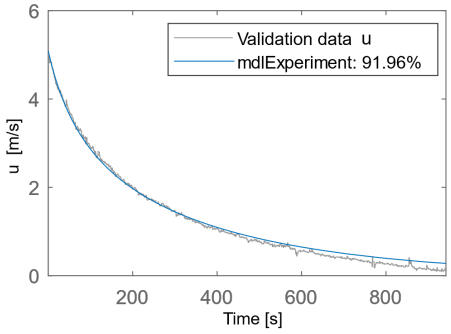

Fig. 3. Comparison of measured and approximated data of a coast stop maneuver only with pump-jet

B. Wind Model

Nowadays, it is common to use existing ship models of similar size and shape when developing a wind model. The vector of the wind forces and moment is defined by

$$\boldsymbol{\tau}_{wind} = \begin{pmatrix} X_{wind} \\ Y_{wind} \\ N_{wind} \end{pmatrix} = \begin{pmatrix} A_F c_X(\alpha) \\ A_L c_Y(\alpha) \\ L A_L c_N(\alpha) \end{pmatrix} \frac{\rho}{2} v_{wind}^2 \tag{9}$$

where A_F denotes the frontal area and A_L the lateral area over the water, L the length of the vessel, c_X, c_Y and c_N the ship specific shape coefficients in the three DoF, ρ the air density, v_{wind} the wind velocity as well as α the wind angle relative to the ship. Models are mostly developed with scaled model ships from ship testing institutions, e.g [9]. The shape coefficients are a function of the wind angle of attack and the areas are documented. A given wind model can be verified with the commanded values for the virtual forces and moment under DP control. The specific look-up tables of the coefficient are scaled so that actuator and wind forces are in the same frame of reference.

As a reference model for the wind coefficients, the research vessel in [9] was chosen. The profile of the structures on the ship closely resembles that of the *DENEB*, so the model ship examined in the wind tunnel is probably the research vessel. The wind coefficients were validated using the DP control with different angles of attack, varying the heading angle in relation to the wind angle. *DENEB* is equipped with a weather station for wind measurement which is mounted on the main mast near the antenna deck and thus more than 20 m above the CG. On the one hand, the development of the wind model has the advantage that it takes into account the real conditions, which wind strength is measured and which actually attack the relevant areas, but on the other

hand, wind shadows at hull height are never included in measurements. The additional motion of the wind sensor, e.g. the roll motion, due to the distance to the CG is largely eliminated by motion filters. The mean wind speed during the tests was approx. 6 m/s. The applied DP controller was already published in [11].

Fig. 4 shows the results for the coefficient c_Y. The controller output $\boldsymbol{\tau}_{act}$ was used to solve the equation 9 for the coefficients c_X, c_Y and c_N with the assumption, that $\boldsymbol{\tau}_{act} = \boldsymbol{\tau}_{wind}$ during keeping the position. The mean values of the force measurements for different wind angles are the basis for identifying the scaling factor for the original coefficient curves by minimizing the distance to the mean values. The validation results for c_X and c_N are comparable in quality.

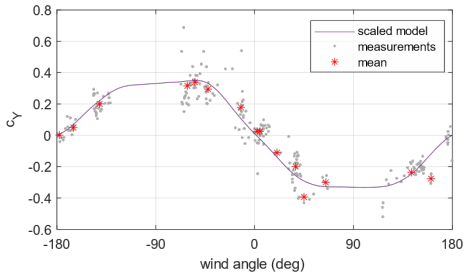

Fig. 4. Validation of the wind coefficient c_Y with the scaled model from [9], the measurements and the calculated mean values

C. Model for power consumption

The power consumption of an engine depends on the applied revolution speed and the generated moment. But there are many other influencing factors, such as the current state of motion of the vehicle and propulsion unit, the dynamic of these two processes, whether the speed is decreasing or increasing, and the thermodynamic processes in the background. In addition, most values are usually not measurable onboard conventional vessels. The models used here are rough estimates based on current revolution speed only. A third-order polynomial was used for each actuator to describe the power consumption during maneuvering in port. A detailed description of this research is found in [12].

For the research vessel *DENEB*, the models for the power consumption of the corresponding actuator as a function of the revolution speed respectively the EOT value are given with

$$\begin{aligned} P_M &= 4.094 \cdot 10^{-02} \cdot |e_M|^3 \\ P_{PJ} &= 1.042 \cdot 10^{-04} \cdot |e_{PJ}|^3 \\ P_T &= 7.928 \cdot 10^{-05} \cdot |e_T|^3 \end{aligned} \tag{10}$$

where P denotes the power measured in Ws for the main propulsion M, pump-jet PJ and stern thruster T.

D. Simulation environment

The developed models are arranged into a comprehensive simulation model using Simulink® according to Fig. 1 to simulate the power or energy consumption for the research vessel under different wind speeds and angles of attack. The wind is assumed to be a constant wind field for the simulations. Such constant values do not occur in the real world, but for a rough estimate of energy consumption this assumption is sufficient.

The first test was restricted to the force component X generated by the main propulsion only. The wind angle was set to constant 0 deg in earth-fixed coordinates as was the heading angle. Both the manipulated variable for the main propulsion e_M and the wind speed v_{wind} were simulated for the respective range and the steady-state velocity u was determined. From the stationary power demand, the energy consumption is calculated, that is needed to sail a distance of 100 m with this constant velocity.

The second simulation sequence quantifies the power required to maintain heading angle ψ and velocity u under the influence of wind. For this reason, the simulation model was combined with a proportional-integral (PI) or a proportional-integral-derivative (PID) controller, as shown in Fig. 5, to avoid a steady-state error and estimate the stationary surge velocity and corresponding revolution speed of the main propulsion. The heading angle is kept at 0 deg in earth-fixed coordinates while the commanded surge velocity is varied in each simulation sequence. The attacking wind is varied in a speed range of $[1, 10]$ m/s and a angle range of $[0, 2\pi]$.

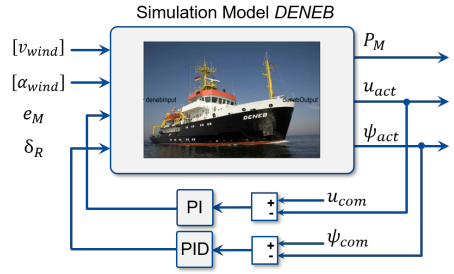

Fig. 5. Struture of the surge and heading control with the simulation model

III. RESULTS AND DISCUSSION

The quality of the model is illustrated with the comparison between the measurement data and simulation output, seen in Fig. 6. In each diagram, the measured and simulated results, with and without wind disturbance, are plotted. A berthing maneuver was performed by a younger and thus less experienced nautical officer in port of Rostock under mean, absolute wind conditions of 4.7 m/s from -54 deg. In this moderate conditions, the controllability of the vessel is not compromised even at slow speeds. The recorded actuator settings and wind measurements were used as input into the simulation model presented in Fig. 1. Vectors of the state variables and the calculated power consumption of the actuators are the simulation output. In the beginning, the vessel

accelerates in a straight line by using the main propulsion and rudder. Then a course changing follows, after 300 s, and the final position is reached by using pump-jet and thruster, from about 450 s. During the curve sailing, the highest difference between measured and modeled lateral velocity v is found. The quality of the models was evaluated using the performance index defined as

$$J = \frac{1}{n}\sum_{k=1}^{n}\left(\left(\frac{\Delta u_k}{u_{max}}\right)^2 + \left(\frac{\Delta v_k}{v_{max}}\right)^2 + \left(\frac{\Delta r_k}{r_{max}}\right)^2\right) \quad (11)$$

where n is the number of samples analyzed, Δu_k, Δv_k and Δr_k are the differences between the measured and simulated state variable in each sample, and u_{max}, v_{max} and r_{max} are the absolute maximum values of measured state variables within the analyzed interval. The time interval of the example was 720 s with a sample time of 0.01 s. For the simulation without the wind disturbances, the performance index is 0.36 and with the consideration of the wind, it is 0.055, which confirms a significantly better performance.

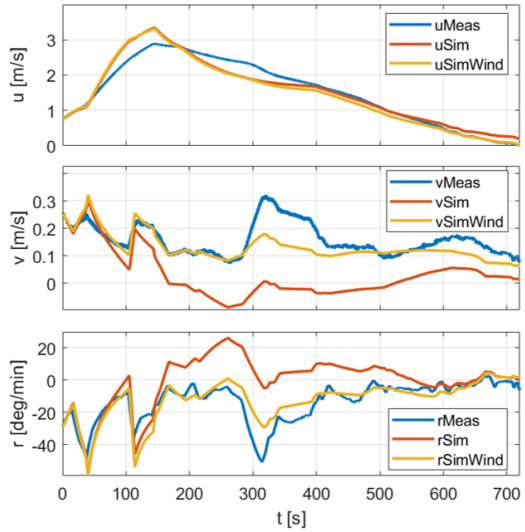

Fig. 6. Comparison for u, v, and r between measurement data and simulation output with and without consideration of the wind

As an example, Fig. 7 shows the power consumption of the pump-jet in comparison of measurement data and simulation out. The simulation model does not represent the transient or internal engine states. The number of changing the actuator command is very high during manual maneuvering. Therefore, the energy consumption of the pump-jet was underestimated with 8 % and for the thruster with 17 % in the model. The estimations for the main propulsion were too high at 18 %, where there is probably a stronger dependence on the velocity u. The power decreases at a constant revolution speed when the stationary state is reached.

In a second step, the simulation model reduced to the motion in the x-direction was used to determine the required power in the steady-state for different wind

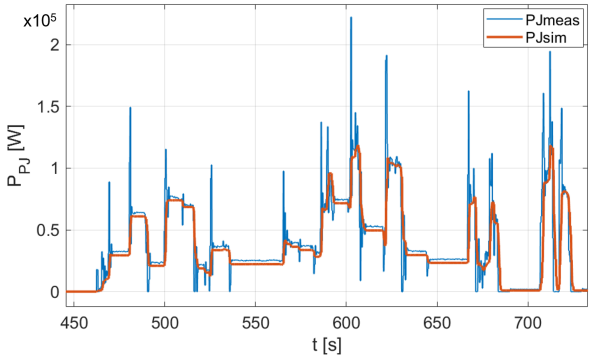

Fig. 7. Comparison for power consumption of the pump-jet between measurement data and simulation output

speeds from the front and set-points of e_M for the main propulsion. The energy required for an exemplary distance of 100 m is calculated with

$$E_M = \frac{P_M \cdot 100}{u_{stat}} \quad (12)$$

where u_{stat} denotes the steady-state surge velocity. Fig. 8 presents the results. The achieved surge velocities are represented in the ordinate. The lower curve shows the simulation results for a wind speed of 1 m/s and the upper curve those for 10 m/s. While the curves hardly differ at higher speeds, there are large differences in the range up to approx. 2 m/s. The minimum energy consumption drifts for higher wind speeds to higher surge velocities. At a speed of 10 m/s, the minimum energy lies at 1.2 m/s, while at a wind speed of 6 m/s it is at 0.8 m/s. where the energy consumption is being only 36 % of this at 10 m/s. If at a wind speed of 6 m/s the surge is reduced from 2 to 1 m/s, the energy consumption is reduced by 58 % while it doubles the time required.

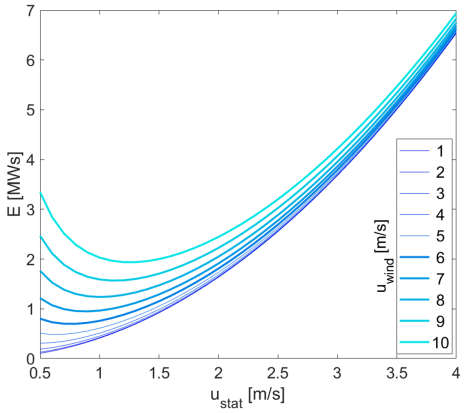

Fig. 8. Energy consumption for a distance of 100 m with variations of u_{wind} from 0 deg and the steady-state surge velocity u_{stat}

The polar plot in Fig. 9 shows the power demand for a controlled surge velocity of 3 m/s and heading angle of 0 deg at different wind speeds and angles of attack represented as longitudinal and transverse velocity components. At this velocity, the motion of the vessel

is good controllable only with the main propulsion and rudder, so that commanded values were kept at all wind conditions. It is clear that wind from behind reduces the power requirement and wind from the front increases it. But the application of the *DENEB* specific wind model shows, that the maximum power is required with wind from -26 *deg* and the minimum with wind from 159 *deg*. The maximum needed power at a wind speed of 10 m/s is about 14 % of the maximum achievable power for the main propulsion at a revolution speed of 51 %. Thus, with the newly developed model, it is possible to calculate maximum allowed actuator commands or the feasibility of a maneuver from given power or energy reserves and environmental conditions. This knowledge can be used in future developments of energetically optimized maneuver strategies.

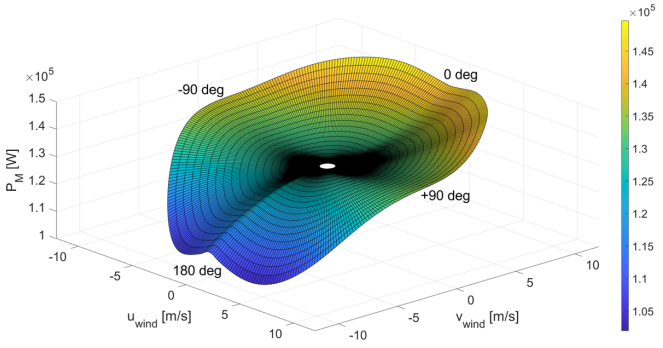

Fig. 9. Power demand of the main propulsion with variations of longitudinal and transverse wind components u_{wind} and v_{wind} under feedback control of velocity u and heading angle ψ

IV. CONCLUSIONS AND OUTLOOK

It was shown that inclusion of actual wind forces improves the motion model of a maneuvering vessel. The energy required for a particular route is also based on models of actuator forces and power consumption. In addition, it was found that the surge velocity, which leads to minimum power consumption during maneuvering, depends on the current wind conditions.

The improved model is intended to be used for automatic maneuvering within safety-critical areas, such as cooperative maneuvering or automatic berthing. It can be included in the maneuver planning and the online optimization during execution of maneuvers. Future developments aim at automatic trajectory planning according the current external conditions in order to minimize the energy consumption of the maneuver. The influence of other external forces on the ship's motion due to the current or interaction with port facilities should be investigated.

ACKNOWLEDGMENT

The authors would like to thank the German Federal Maritime and Hydrographic Agency (BSH) for making these tests on the survey and research vessel *DENEB* possible. Our special thanks also go to the *DENEB* crew, who not only supported us with unwavering calm, but contributed significantly to the success of these tests.

REFERENCES

[1] E. Bouman, E. Lindstad, A. Rialland, A. Stromman, "State-of-the-art technologies, measures, and potential for reducing GHG emissions from shipping – a review," Transp Res Part D, 52:408–421, 2017

[2] M. Bentin, D. Zastrau, M. Schlaak, D. Freye, R. Elsner, S. Kotzur, "A new routing optimization tool-influence of wind and waves on fuel consumption of ships with and without wind assisted ship propulsion systems," Transportation Research Procedia, 14,pp. 153 – 162, 2016.

[3] G. Finger, M. Schaub, F. Dahms, E. Hassel, T. Riebe, G. Milbradt, and K. Wehner, "On-Board Support System for the eco-friendly ship operation in coastal and port areas," in Proceedings of OCEANS 2019, Marseille, France, 2019.

[4] T. Suzuki, "Challenge of technology development through MEGURI 2040 - For safe navigation and workload reduction," ClassNK Technical Journal, No. 3, pp. 51-58, 2021.

[5] R. Sawada, K. Hirata, Y. Kitagawa, E. Saito, M. Ueno, K. Tanizawa, J. Fukuto, "Path following algorithm application to automatic berthing control," Journal of Marine Science and Technology, Vol. 26, pp.541-554, 2021.

[6] Y.A. Ahmed, K. Hasegawa, "Consistently Trained Artificial Neural Network for Automatic Ship Berthing Control," TransNav - International Journal on Marine Navigation and Safety of Sea Transportation, Vol. 9(13), pp.417-426, 2015.

[7] N.-K. Im, V.-L. Tran, "Ship's Maneuverability in Strong Wind," Journal of Navigation and Port Research, Vol.32 (2), pp.115-120, 2008.

[8] T.I. Fossen, "Handbook of Marine Craft Hydrodynamics and Motion Control," John Wiley & Sons, Ltd, 2011.

[9] W. Blendermann, "Schiffsform und Windlast-Korrelations- und Regressionsanalyse von Windkanalmessungen am Modell (Correlation and regression analysis of ship hull and wind load of wind tunnel measurements with models)," University of Hamburg, Institute of Shipbuilding, Series of publications shipbuilding (Schriftenreihe Schiffbau), 533, March 1993.

[10] C. Rethfeldt, A.U. Schubert, R. Damerius, M. Kurowski, and T. Jeinsch,"System Approach for Highly Automated Manoeuvring with Research Vessel DENEB," Proceedings of 13th IFAC Conference on Control Applications in Marine Systems, Robotics, and Vehicles (CAMS), pp. 1–6, Oldenburg, Germany, 2021.

[11] T. Hahn, R. Damerius, C. Rethfeldt, A.U. Schubert, M. Kurowski, T. Jeinsch, "Automated maneuvering using model-based control as key to autonomous shipping," at - Automatisierungstechnik, 70 (5), pp.456–468, 2022.

[12] R. Damerius, A.U. Schubert, C. Rethfeldt, G. Finger, S. Fischer, G. Milbradt, M. Kurowski, M. Gluch, T. Jeinsch,"Consumption-reduced manual and automatic manoeuvring with conventional vessels," Journal of Marine Engineering and Technology, 22:2, pp. 55-66, 2022.